REGULAR ARTICLE

blood advances

Yin Yang 1 regulates cohesin complex protein SMC3 in mouse hematopoietic stem cells

Zhanping Lu,[1-3,*] Yinghua Wang,[1-3,*] Anna L. F. V. Assumpção,[1-3,*] Peng Liu,[2,4] Audrey Kopp,[3,5] Sahitya Saka,[1-3] Sean J. Mcilwain,[2,4] Aaron D. Viny,[6-8] Marjorie Brand,[3,5] and Xuan Pan[1-3]

[1]Department of Medical Sciences, School of Veterinary Medicine, University of Wisconsin, Madison, WI; [2]Carbone Cancer Center and [3]Wisconsin Blood Cancer Research Institute, University of Wisconsin, Madison, WI; [4]Department of Biostatistics and Medical Informatics and [5]Department of Cell and Regenerative Biology, University of Wisconsin School of Medicine and Public Health, Madison, WI; [6]Division of Hematology & Oncology, Department of Medicine, [7]Columbia Stem Cell Initiative, and [8]Department of Genetics & Development, Columbia University Irving Medical Center, New York, NY

Key Points

- YY1 cooccupies with SMC3 at a large cohort of promoters genome wide and represses SMC3 expression in HSPCs.
- Establish a distinct regulatory circuit of 2 chromatin structural factors and its impact on HSC quiescence and metabolism.

Yin Yang 1 (YY1) and structural maintenance of chromosomes 3 (SMC3) are 2 critical chromatin structural factors that mediate long-distance enhancer-promoter interactions and promote developmentally regulated changes in chromatin architecture in hematopoietic stem/progenitor cells (HSPCs). Although YY1 has critical functions in promoting hematopoietic stem cell (HSC) self-renewal and maintaining HSC quiescence, SMC3 is required for proper myeloid lineage differentiation. However, many questions remain unanswered regarding how YY1 and SMC3 interact with each other and affect hematopoiesis. We found that YY1 physically interacts with SMC3 and cooccupies with SMC3 at a large cohort of promoters genome wide, and YY1 deficiency deregulates the genetic network governing cell metabolism. YY1 occupies the *Smc3* promoter and represses SMC3 expression in HSPCs. Although deletion of 1 *Smc3* allele partially restores HSC numbers and quiescence in YY1 knockout mice, $Yy1^{-/-}$ $Smc3^{+/-}$ HSCs fail to reconstitute blood after bone marrow transplant. YY1 regulates HSC metabolic pathways and maintains proper intracellular reactive oxygen species levels in HSCs, and this regulation is independent of the YY1–SMC3 axis. Our results establish a distinct YY1–SMC3 axis and its impact on HSC quiescence and metabolism.

Introduction

Yin Yang 1 (YY1) is a ubiquitous zinc finger transcription factor and polycomb group protein (PcG) that can activate or repress transcription of target genes,[1,2] promote chromatin/chromosome structural changes, and form gene-regulatory DNA loops between proximal and distal promoters and enhancer binding sites through homodimer interactions.[3,4] YY1 orchestrates PcG-mediated gene repression by recruiting other PcG members to specific chromatin sites to control histone modifications.[5-7] YY1 plays important roles in gene regulation, early embryonic development, X-chromosome inactivation, DNA repair, normal hematopoiesis, as well as hematopoietic cancers.[8-11] Although YY1 is required for both B- and T-lymphocyte development,[8,12-16] its functions in hematopoietic stem cell (HSC) development were incompletely characterized. Our previous study demonstrates that a conditional *Yy1* knockout in

Submitted 9 August 2023; accepted 26 February 2024; prepublished online on *Blood Advances* First Edition 26 March 2024. https://doi.org/10.1182/bloodadvances.2023011411.

*Z.L., Y.W., and A.L.F.V.A. contributed equally to this work.

The data sets generated and/or analyzed during this study are available on reasonable request from the corresponding author, Xuan Pan (xpan24@wisc.edu).

The full-text version of this article contains a data supplement.

HSCs decreases long-term repopulating activity, and that ectopic YY1 expression expands HSCs. YY1 deficiency deregulates the genetic network governing HSC proliferation, impairs stem cell factor/c-Kit signaling, and disrupts mechanisms conferring HSC quiescence.[17] Nevertheless, the underlying mechanisms by which YY1 regulates HSC quiescence and self-renewal are still largely unknown.

Cohesin is a multimeric protein complex that is important for sister chromatid cohesion and segregation during mitosis. Cohesin consists of a ring-like structure comprised of structural maintenance of chromosomes (SMC)1, SMC3, and RAD21, bound to STAG1 or STAG2, which wraps around chromatin.[18,19] SMC1 and SMC3 form the core component of the cohesin complex.[19] Cohesin encircles chromatin fibers without directly binding to DNA and plays critical roles in chromosome segregation, DNA repair, and DNA looping.[20-22] Depletion of cohesin core components promotes HSC expansion to skew toward myeloid differentiation.[23-26] Homozygous deletion of *Smc3* causes bone marrow (BM) aplasia in mice and SMC3-deficient mice die shortly. *Smc3* haploinsufficiency increases HSC self-renewal and cooperates with myeloid leukemia oncogene *Flt3*-internal tandem duplications to induce acute myeloid leukemia.[26] Knockdown of cohesin complex proteins by short hairpin RNA (shRNA) can lead to myeloproliferative neoplasms in mice.[23]

Enhancers and gene promoters interact with each other to regulate the expression of target genes. An established paradigm for enhancer function involves chromatin looping in which the 2 sites are brought physically close together.[27-30] Proteins that facilitate chromatin looping alter local and higher-order chromatin structure, and therefore these proteins are defined as chromatin structural factors. YY1, cohesion, and CCCTC-binding factor (CTCF) are all essential chromatin structural factors.[3,4,22,31-35] In addition, YY1 and cohesin complex proteins are critical for regulating HSC fate.[23-26,35] Many questions remain unanswered regarding how chromatin structural factors interact with each other and impact hematopoiesis. Our RNA-sequencing (RNA-seq) analysis comparing wild-type and $Yy1^{-/-}$ HSCs demonstrated that *Smc3* is upregulated in YY1-deficient cells, and genes regulated by YY1 are significantly enriched in cell cycle progression, cell division, chromosome condensation and segregation, and cytoskeleton and spindle organization.[17] Thus, we hypothesized that YY1 is a critical regulator of the cohesin complex protein SMC3, and that there is a distinct YY1–SMC3 axis-dependent/-independent regulation of HSC functions.

Herein, we demonstrate that YY1 and cohesin complex proteins cooccupy a large cohort of promoters genome wide by physically interacting with the cohesin protein SMC3. YY1 deficiency deregulates the genetic network governing cell metabolism. YY1 represses SMC3 expression and occupies the *Smc3* promoter in hematopoietic stem and progenitor cells (HSPCs). Although SMC3 is upregulated in YY1-null BM cells (BMCs), SMC3 protein expression was normalized in $Yy1^{-/-}$ $Smc3^{+/-}$ cells. Although deletion of 1 *Smc3* allele partially rescues long-term HSC (LT-HSC) percentage in YY1-deficient mice and leads to a partial restoration of HSC quiescence, $Yy1^{-/-}Smc3^{+/-}$ cells fail to reconstitute blood in mice that received BM transplantation. YY1-deficient HSCs have increased intracellular reactive oxygen species (ROS) levels, and the regulation of proper ROS level is independent of the YY1–SMC3 axis. Our results establish a distinct regulatory circuit of 2 chromatin structural factors and its impact on HSC quiescence and metabolism.

Methods

ChIP-seq data analysis

Chromatin immunoprecipitation sequencing (ChIP-seq) data for CTCF, H3K27ac, SMC1, SMC3, and YY1 as well as associated input were downloaded from Gene Expression Omnibus (GEO; accession identifiers: GSE22562, GSE62380, and GSE68195).[36-38] ENCyclopedia Of DNA Elements (ENCODE) ChIP-seq pipeline (version 2.1.6) was used to align reads to mouse genome (mm10) and call peaks. Protein-coding transcripts and long noncoding RNAs from GENCODE basic annotation (version M22) were used to define exons and introns. Proximal promoter is defined as 1 kb upstream of a gene, and distal promoter is defined as 4 kb upstream of a proximal promoter. H3K27ac peaks were considered as enhancers and the rest of the genomic regions were defined as intergenic. The genomic locations of ChIP-seq peaks from chromosomes 1 to 19 and X are determined by peak overlap with the aforementioned 6 types of genomic regions. Gene Ontology (GO) term overrepresentation was analyzed by the goana function from the Bioconductor package limma (version 3.50.1).

Cleavage under targets and tagmentation analysis

According to published protocol[39] (see supplemental Material for details), the cleavage under targets and tagmentation (CUT&Tag) libraries were constructed with hematopoietic precursor cell-7 (HPC-7) cells infected with MigR1-shLuc or MigR1-shYY1. CUT&Tag FASTQ files were first processed by removing the adapter "CTGTCTCTTATACACATCT" using the Cutadapt software (version 4.5) and then aligned to the mouse genome (version mm10) by Bowtie2 (version 2.5.1). Duplicated fragments were marked and removed by Picard (version 3.1.1). Peaks were called by MACS2 (version 2.2.9.1) for each replicate under a q-value cutoff of 10^{-6}. Only peaks from chromosome 1 through 19, X, or Y, and not overlapping with any of the ENCODE problematic genomic regions (https://www.encodeproject.org/files/ENCFF547MET/) were kept. Because every sample has 3 replicates, we defined peaks for a sample as the genomic regions belonging to peaks called in all 3 replicates and with a minimum genomic span of 10 base pairs (bp). Peak location type and GO term overrepresentation were processed in the same way as in ChIP-seq analysis.

Mice

To induce the expression of cyclization recombinase (Cre), 8-week-old mice were injected with 100 μg of pI-pC (GE Healthcare Life Science) every other day for 4 doses. Approximately equal proportions of male and female mice were used, and aggregated data were presented because sex-specific differences were not found (supplemental Figure 9). All experiments described in this manuscript were performed 7 days after the last injection of pI-pC, unless stated otherwise. All experiments involving mice were approved by the institutional laboratory animal care and use committee of the University of Wisconsin-Madison and conform to the appropriate regulatory standards.

BM transplantation

Competitive BM transplantation assay was performed as previously described.[17] Total BMCs were transplanted to lethally irradiated (8.5 Gy) recipient mice (CD45.1$^+$). At 4 week after transplantation, recipient mice were treated with 4 doses of pI-pC every other day. Peripheral blood chimerism was evaluated by flow cytometry every 4 weeks.

Flow cytometric analysis

Directly conjugated or biotin-conjugated antibodies specific for the following surface antigens were purchased from eBioscience: CD3 (145-2C11), CD4 (RM4-5), CD8 (53-6.7), B220 (RA3-6B2), TER119 (TER-119), Gr-1 (RB6-8C5), IgM (eB121-15F9), CD19 (eBio1D3), interleukin 7Rα (A7R34), CD45.2 (104), CD45.1 (A20), Sca1 (D7), c-Kit (2B8), Mac1 (M1/70), and Thy1.2 (53-2.1). CD48 (103427) and CD150 (TC15-12F12.2) were purchased from BioLegend. Ghostdye Violet510 (Tonbo Bioscience) was used to exclude nonviable cells. Data were acquired from LSR Fortessa (BD Biosciences) and analyzed using BD FlowJo version 10.0.7 software.

Cell cycle analyses

BMCs were fixed with 4% paraformaldehyde, permeabilized with 0.1% saponin in phosphate-buffered saline, and stained with fluorescein isothiocyanate–conjugated Ki67 (BD Biosciences) and DAPI (4′,6-diamidino-2-phenylindole; Thermo Fisher) in addition to HSC, Lin$^-$ Sca1$^+$c-kit$^+$ (LSK), myeloid progenitors (MP; Lin$^-$ Sca1$^-$c-kit$^+$), and multipotent progenitor (MPP) markers.

RNA-seq data analysis

RNA-seq reads were aligned by Spliced Transcripts Alignment to a Reference (version 2.5.2b) to the mouse genome (version mm10) with GENCODE basic gene annotations (version M22). Gene expression levels were quantified by RNA-Seq by Expectation-Maximization (version 1.3.0), and differential expression was analyzed by edgeR (version 3.36.0). A differentially expressed gene was required to have at least twofold changes, an adjusted P value $< .05$, and transcript per million ≥ 1 in all the replicates in at least 1 of 2 conditions in comparison. Gene set enrichment analysis was performed by fgsea (version 1.20.0) with M2 curated gene sets from the Molecular Signatures database (version 2022.1.Mm). The RNA-seq data have been deposited to GEO with an access identity GSE239743 (https://www.ncbi.nlm.nih.gov/geo/query/acc.cgi?acc=GSE239743) and a secure token, yrsruwgurxgjfqh.

Statistical analysis

All statistical analyses were conducted using GraphPad Prism version 7.04. The Student t test was used to determine statistical significance between *Mx1-Cre* and *Yy1$^{f/f}$Mx1-Cre* groups. Differences between the 4 groups were determined using a 1-way analysis of variance followed by Tukey post hoc test. Two-way analysis of variance followed by Tukey post hoc test was used to compare cells in different phases of the cell cycle, as measured by Ki67 and DAPI flow cytometry analysis. P values $\leq .05$ were considered statistically significant.

Results

YY1 and cohesin complex proteins cooccupy a large cohort of promoters genome wide

To assess YY1 and cohesin complex proteins SMC3 and SMC1A binding sites throughout the genome, previously published ChIP-seq data sets on mouse embryonic stem cells from GEO under the accession GSE62380, GSE68195, and GSE22562 were analyzed.[36-38] In total, 20 154 SMC3 ChIP-seq peaks were identified and stratified by their genomic locations. CTCF, SMC1, and YY1 binding peaks had overall strong overlapping with SMC3 peaks at all genomic locations (Figure 1A; supplemental Figure 1). Among the 20 154 SMC3 peaks, >90% of SMC3 binding peaks were cooccupied with CTCF, SMC1, and/or YY1, with only 1528 SMC3 peaks were not. At most of the genomic locations, SMC3 colocalized more frequently with CTCF and SMC1 than YY1 (Figure 1A-B). YY1 cooccupancy with cohesin and CTCF is more prevalent in the proximal promoter compared with other genome locations. Overall, 32% of SMC3 binding peaks at the proximal promoter were cooccupied with YY1, CTCF, and SMC1 compared with 19.1% at the enhancer, 16.1% at the exon, 13% at the distal promoter, 10.1% at the intron, and 6% at the intergenic region (Figure 1B). Interestingly, GO term overrepresentation analysis on genes cooccupied by cohesin, CTCF, and/or YY1 at proximal promoters indicated a functional significance of YY1 dependent vs independent regulation at proximal promoters. For promoters with YY1-independent cohesion-CTCF occupancy, genes were enriched in cellular differentiation and developmental process (Figure 1C). In contrast, for promoters with YY1-dependent occupancy, genes were mainly enriched in the metabolic process (Figure 1D).

To further evaluate YY1 and SMC3 cooccupancy in HSPCs, we conducted CUT&Tag experiments in the HSPC line HPC-7[40,41] with antibodies against YY1 and SMC3. Consistent with compiled ChIP-seq data (Figure 1), YY1 had strong overlapping with SMC3 peaks at all genomic locations (Figure 2; supplemental Figure 2). Among 1824 SMC3 binding peaks, 83% were cooccupied by YY1. Among 3602 YY1 binding peaks, 42% were cooccupied by SMC3 (Figure 2B). YY1 cooccupancy with SMC3 is more prevalent in the proximal promoter than other genome locations. Of cobinding peaks, 56% were at the proximal promoter compared with 25% at intron, 9% at exon, 8% at intergenic region, and 1.6% at the distal promoter (Figure 2C). YY1 activates c-Kit expression in HSPCs by binding at the *Kit* locus.[17] The CUT&Tag analysis revealed a YY1-SMC3 cobinding peak at the *Kit* locus. Upon YY1 knockdown, YY1 enrichment at the *Kit* locus was reduced, whereas SMC3 binding was intact (supplemental Figure 2D). Consistent with compiled ChIP-seq data (Figure 1D), GO term overrepresentation analysis on genes cooccupied by YY1 and SMC3 at the proximal promoter region show that top 10 enriched pathways are involved in cell metabolism (Figure 2D). To determine what overlapping cobinding sites of YY1 and SMC3 depend on the presence of YY1, we knocked down YY1 in HPC-7 cells by shRNA. Over 70% of *Yy1* transcript was reduced in HPC-7 cells infected with sh-YY1 vs sh-Luc (supplemental Figure 8). Peak analysis in YY1 knockdown HPC-7 cells show that ~27% of SMC3 binding peaks were lost upon YY1 knockdown (Figure 2E), most of which were associated with genes that are critical for cell metabolic process (Figure 2F). The ChIP-seq and CUT&Tag assays support that YY1 and SMC3 cooccupy at proximal promoter regions that are critical for regulating cellular metabolism.

YY1 physically interacts with SMC3 via its zinc finger domain

Because YY1 and cohesin complex proteins cooccupied a large cohort of promoters throughout the genome, we assessed whether

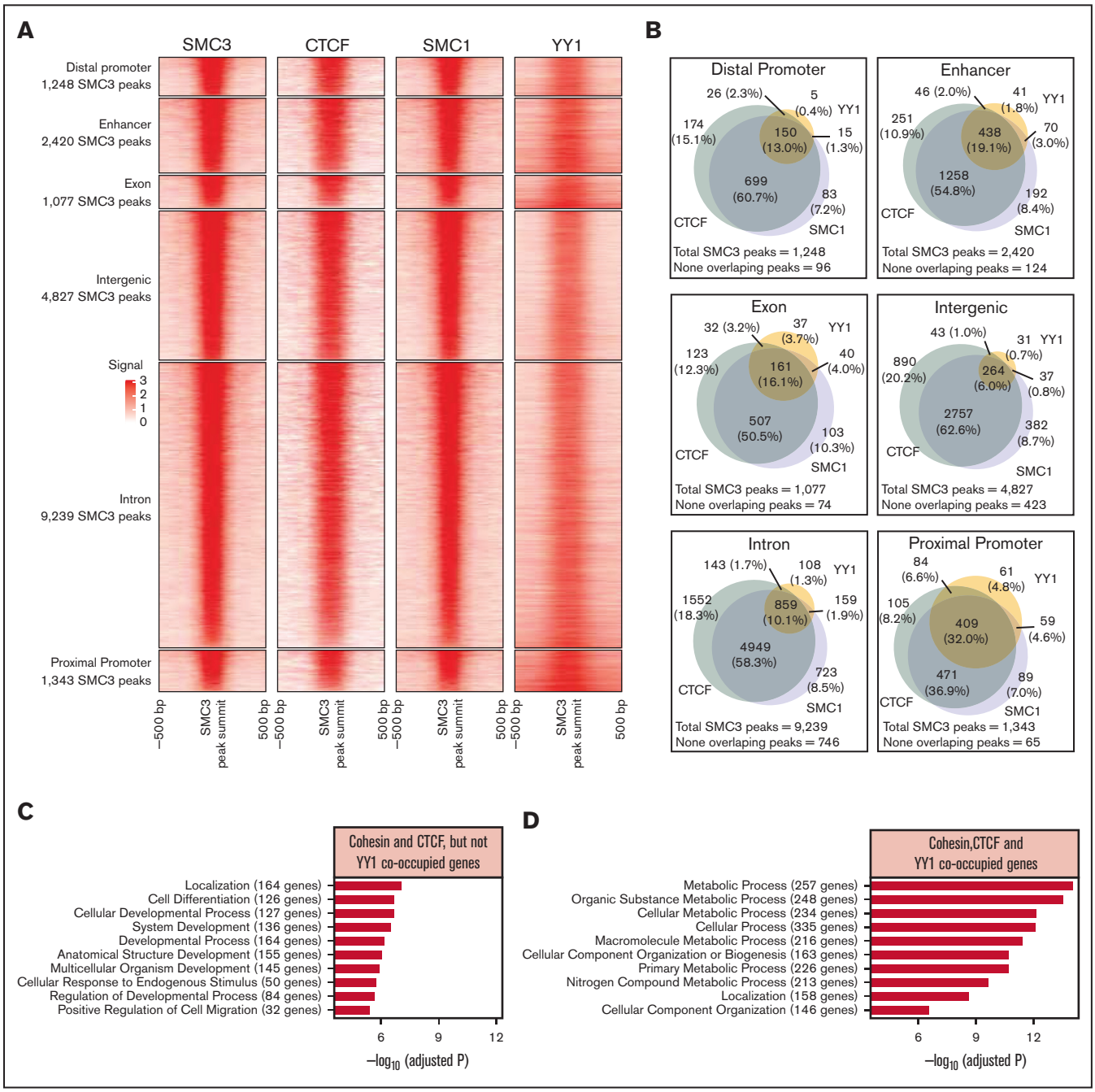

Figure 1. ChIP-seq analysis of YY1 and cohesin complex protein binding sites. (A) Heat map of SMC3, CTCF, SMC1, and YY1 ChIP-seq signals around SMC3 peak summits. Each row represents a SMC3 peak region that is defined as a 500-bp genomic region flanking a SMC3 ChIP-seq peak summit. (B) Venn diagrams to compare the overlapping of CTCF, SMC1, and YY1 peaks with that of SMC3 peaks. (C-D) Top 10 overrepresented GO terms on genes that have proximal promoters overlapping with SMC3 peaks. Genes were stratified by the 471 SMC3 peaks overlapping with SMC1 and CTCF but not YY1 (C), and the 409 SMC3 peaks overlapping with SMC1, CTCF, and YY1 (D).

YY1 physically interacted with cohesin complex proteins. Human embryonic kidney-293 (HEK-293) cells (Figure 3A-B) and HPC-7 cells (Figure 3C-D) were transfected and infected respectively with plasmids expressing Flag-tagged YY1, and the nuclear extracts were coimmunoprecipitated with anti-Flag antibody or immunoglobulin G (IgG) control. Compared with IgG control, cohesin complex proteins SMC1A, SMC3, and RAD21 coimmunoprecipitated when using the anti-Flag antibody in HEK-293 (Figure 3A) and HPC-7 cells (Figure 3C). The reciprocal intraperitoneal co-(IP) was conducted by immunoprecipitation with an anti-SMC3 antibody. Compared with IgG control, YY1 coimmunoprecipitated with anti-SMC3 antibody in HEK-293 (Figure 3B) and HPC-7 cells (Figure 3D). To access endogenous YY1 interaction with SMC3, total BMCs were harvested from C57BL/6 mice at 4 days after 5-fluorouracil injections

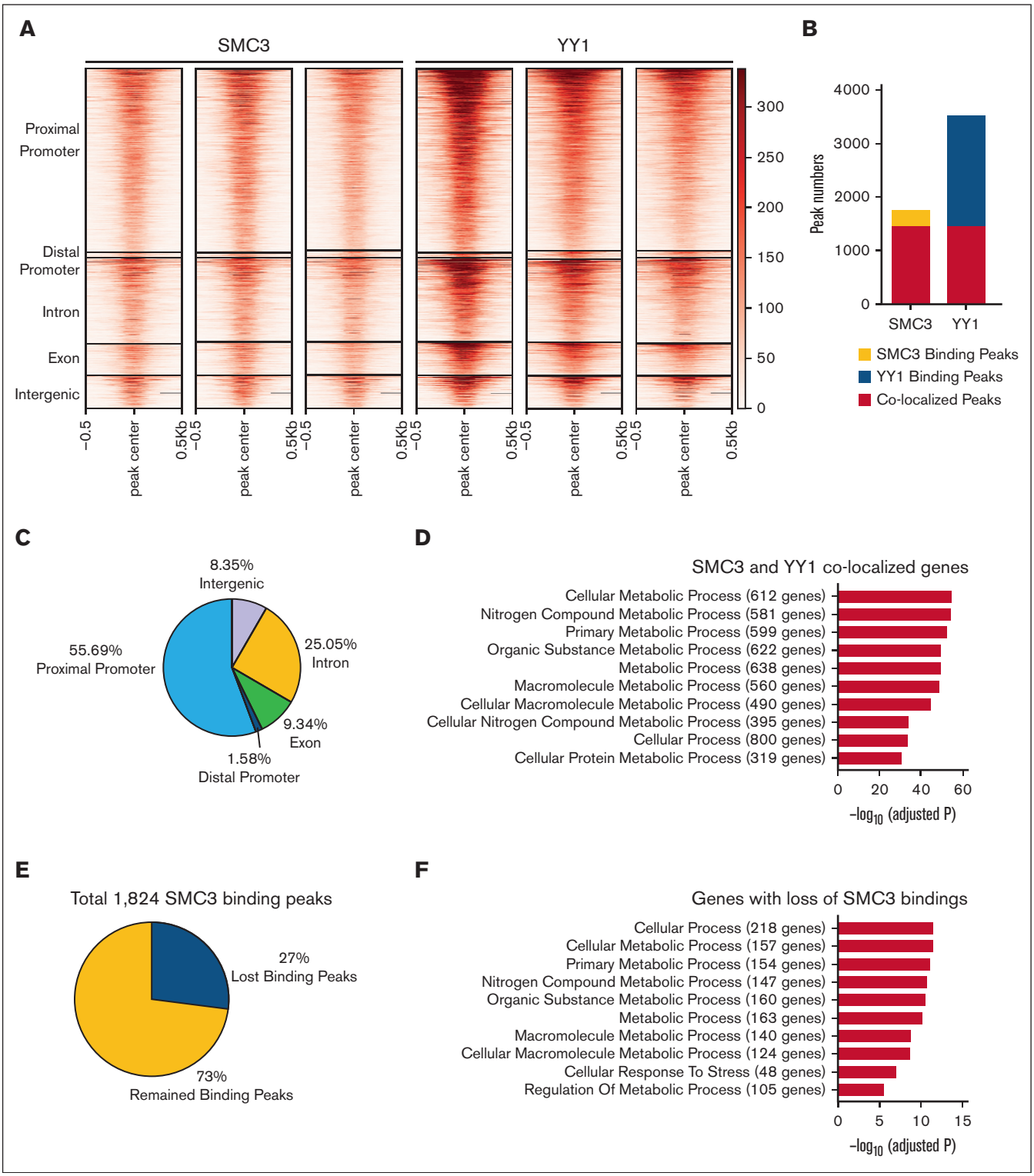

Figure 2. CUT&Tag analysis of YY1 and SMC3 binding sites. (A) Heat map of SMC3 and YY1 signals around SMC3 peak summits at different genomic regions. Each row represents a SMC3 peak region that is defined as a 1-kilobase genomic region flanking a SMC3 CUT&Tag peak summit. (B) YY1, SMC3, and cobinding peak numbers. (C) Percentages and numbers of YY1 and SMC3 cobinding peaks at different genomic regions. (D) Top 10 overrepresented GO terms on genes that have proximal promoters occupied with SMC3 and YY1 peaks. (E) In total, 27% of SMC3 binding peaks were lost upon YY1 knockdown. (F) Top 10 overrepresented GO terms on genes that have lost SMC3 bindings at proximal promoters upon YY1 knockdown.

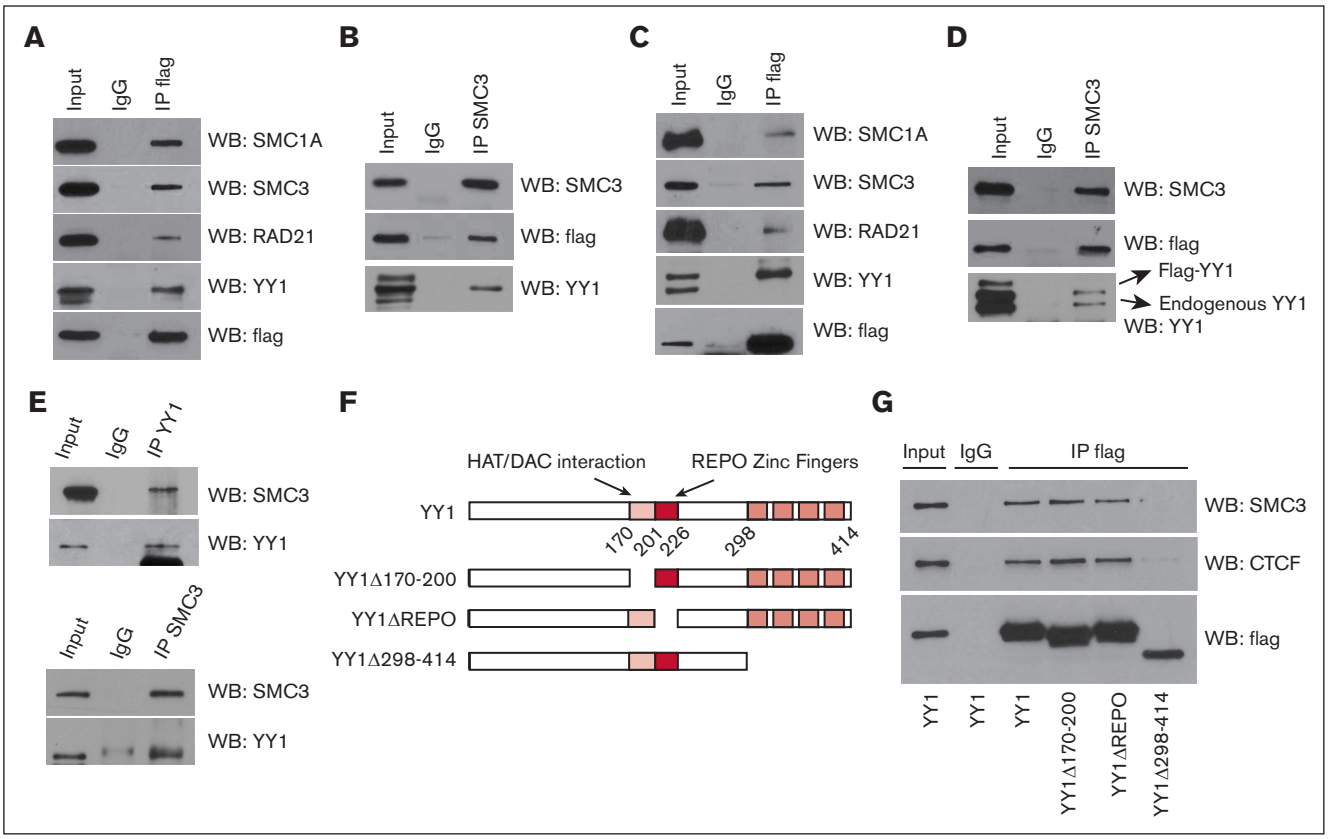

Figure 3. YY1 physically interacts with cohesin complex proteins through its zinc finger domain. (A-B) YY1 physically interacts with cohesin complex proteins in 293 cells. (A) Nuclear extracts were immunoprecipitated with anti-Flag antibody and were western blotted for SMC1A, SMC3, RAD21, YY1, or Flag. (B) Reciprocal nuclear co-immunoprecipitation (co-IP). Nuclear extracts were immunoprecipitated with anti-SMC3 antibody and western blotted for SMC3, Flag, or YY1. (C-D) YY1 physically interacts with cohesin complex proteins in HPC7. (C) Nuclear extracts were immunoprecipitated with anti-Flag antibody and were western blotted for SMC1A, SMC3, RAD21, Flag or YY1. (D) Reciprocal nuclear co-IP. Nuclear extracts were immunoprecipitated with anti-SMC3 antibody and western blotted for SMC3, Flag, or YY1. (E) Endogenous YY1 physically interacts with SMC3 in 5-fluorouracil enriched BMCs. Nuclear extracts of 5-fluorouracil–enriched BMCs from C57BL/6 mice were immunoprecipitated with anti-YY1 or anti-SMC3 antibody and were western blotted for SMC3 or YY1. (F) Diagram of YY1 functional domain and YY1 mutants. (G) YY1 amino acid sequence 298 through 414 is required for its physical interaction with SMC3. Nuclear extracts from transfected cells were immunoprecipitated with anti-Flag antibody and western blotted for SMC3, CTCF, or Flag.

(5 mg/mouse). Endogenous co-IPs were conducted in nuclear extract of 5-fluorouracil–enriched BMCs with IgG control, or anti-YY1 or anti-SMC3 antibody. SMC3 and YY1 proteins coimmunoprecipitated with each other with anti-YY1 (Figure 3E upper panel) or anti-SMC3 antibody (Figure 3E lower panel) in BMCs.

To access which YY1 functional domain is required for its interaction/association with cohesin complex protein SMC3, we transfected HEK-293 cells with wild-type YY1 or YY1 functional domain mutants: YY1 Δ170-200, YY1 ΔREPO, or YY1 Δ298-414. YY1 Δ170-200 deletes a transcriptional repression domain that interacts with numerous proteins[5,42,43]; YY1 ΔREPO deletes the PcG recruiting domain[5]; YY1 Δ298-414 deletes the 4 zinc fingers DNA binding domain[44] (Figure 3F). Although wild-type YY1, YY1 Δ170-200, and YY1 ΔREPO physically interacted with SMC3, YY1 Δ298-414 did not (Figure 3G). Thus, YY1 zinc finger domain is required for YY1 interaction/association with cohesin complex protein SMC3 (Figure 3F-G). We conclude that YY1 and SMC3 occupied a large cohort of the genome by physically interacting with each other.

YY1 occupies the *Smc3* promoter and represses SMC3 expression

Interestingly, compiled ChIP-seq data sets from mouse embryonic stem cells[38] and CUT&Tag data in HPC-7 cells show that YY1 binds strongly at the *Smc3* promoter region (from −389 bp to +416 bp) from transcription start site (Figure 4A; supplemental Figure 3A-B). In contrast, no binding and a weak YY1 binding was detected at the *Smc1* and *Rad 21* promoters respectively (supplemental Figure 3A-B). To assess how YY1 regulates SMC3 expression, we assessed *Smc3* messenger RNA (mRNA) expression by ectopically expressing YY1 in hematopoietic cells. We retrovirally transduced HPC-7[40,41] and total BMCs from B6 mice with MigR1-YY1 vs MigR1 empty vector control. Green fluorescent protein–positive HPC-7 cells and BMCs were sorted by fluorescence-activated cell sorting, and the YY1 expression levels were correlated with the median fluorescence intensity of green fluorescent protein expression (supplemental Figure 3C). Ectopic expression of YY1 in HPC-7 cells and total BMCs led to down-regulation of *Smc3* mRNA expression (Figure 4B) but did not

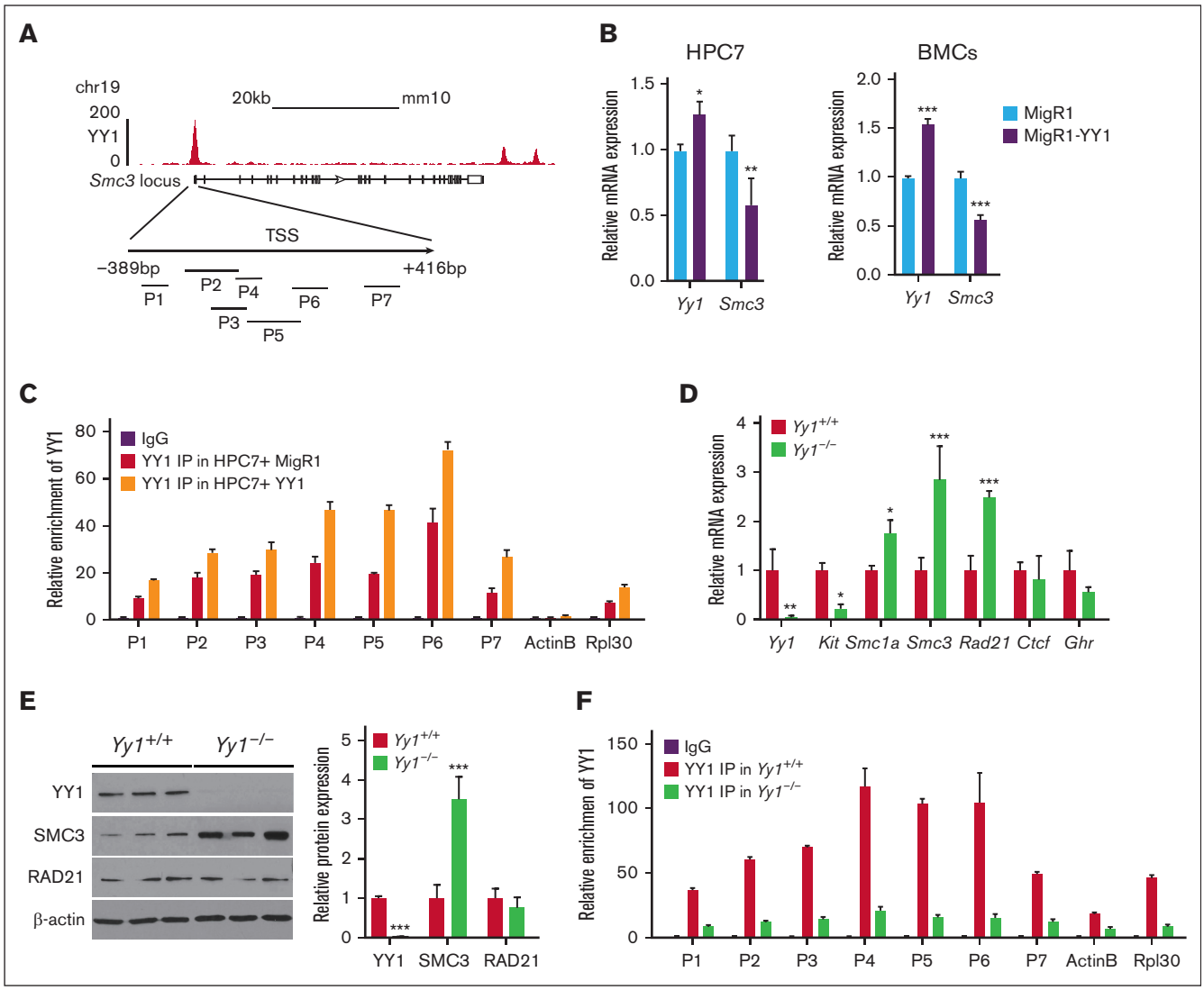

Figure 4. YY1 inhibits SMC3 expression directly. (A) ChIP-seq binding profile for YY1 at the *Smc3* locus in mESCs and YY1 ChIP-qPCR primer design strategy at the *Smc3* promoter (supplemental Figure 10). (B) *Yy1* and *Smc3* transcript levels in HPC7 and total BMCs with and without ectopic YY1 expression. (C) ChIP-qPCR analysis of YY1 bindings at the *Smc3* promoter in HPC7 cells infected with MigR1-YY1 or MigR1 vector only. (D) quantitative reverse transcription PCR to detect transcript levels in Lin$^-$ BMCs of *Yy1*$^{-/-}$and *Yy1*$^{+/+}$ mice. Primers are listed in supplemental Figure 10. (E) Western blot and quantification to detect the YY1, SMC3, and RAD21 protein expressions in total BMCs of *Yy1*$^{-/-}$and *Yy1*$^{+/+}$ mice. (F) ChIP-qPCR analysis of the binding of YY1 at the *Smc3* promoter region in *Yy1*$^{+/+}$ and *Yy1*$^{-/-}$total BMCs. Data are presented as means ± standard deviation (SD); **P* < .05, ***P* < .01, and ****P* < .001.

impact *Smc1* or *Rad 21* mRNA expression (supplemental Figure 3C). To further validate the ChIP-seq and CUT&Tag data, ChIP quantitative polymerase chain reaction (qPCR) was conducted in HPC-7 cells infected with MigR1-YY1 vs MigR1 vector control. We detected the YY1 binding at the *Smc3* promoter, and ectopic expression of YY1 further increased YY1 binding at the promoter region (Figure 4C). These experiments support that YY1 binds at the *Smc3* promoter, and that high YY1 expression suppresses *Smc3* expression at the transcript level in HSPCs. To test how loss of function of YY1 affects SMC3 expression and occupancy, we used a conditional *Yy1*-knockout allele *Yy1*$^{f/f}$ with loxP sites flanking the *Yy1* promoter region and exon1[8] and crossed *Yy1*$^{f/f}$ mice with inducible *Mx1-Cre*. In *Yy1*$^{f/f}$ *Mx1-Cre* mice, YY1 deletion was achieved after treatment with the interferon alfa (IFN-α)-stimulating pI-pC. *Yy1*$^{f/f}$ *Mx1-Cre* (*Yy1*$^{-/-}$) and *Mx1-cre* (*Yy1*$^{+/+}$) mice received 4 doses of pI-pC injections and at 7 days after injections there was a >90% reduction of YY1 mRNA expression in *Yy1*$^{-/-}$ lineage negative (Lin$^-$) BMCs (Figure 4D) compared with *Yy1*$^{+/+}$ Lin$^-$ BMCs. Next, we evaluated *Smc1a*, *Smc3*, and *Rad21* mRNA expressions in *Yy1*$^{-/-}$ vs *Yy1*$^{+/+}$ Lin$^-$ BMCs. Consistent with our previous publication,[17] *Yy1*$^{-/-}$Lin$^-$ cells had decreased *Yy1* and *Kit* mRNA expression compared with *Yy1*$^{+/+}$Lin$^-$ cells, and *Ctcf* and *Ghr* mRNA expression levels were similar. In contrast, *Smc1a*, *Smc3*, and *Rad21* mRNA expressions were significantly increased in *Yy1*$^{-/-}$compared to *Yy1*$^{+/+}$Lin$^-$ BMCs (Figure 4D). In *Yy1*$^{-/-}$ total BMCs, SMC3 protein expression was significantly increased compared with *Yy1*$^{+/+}$ cells, and RAD21 protein expression did not differ significantly (Figure 4E).

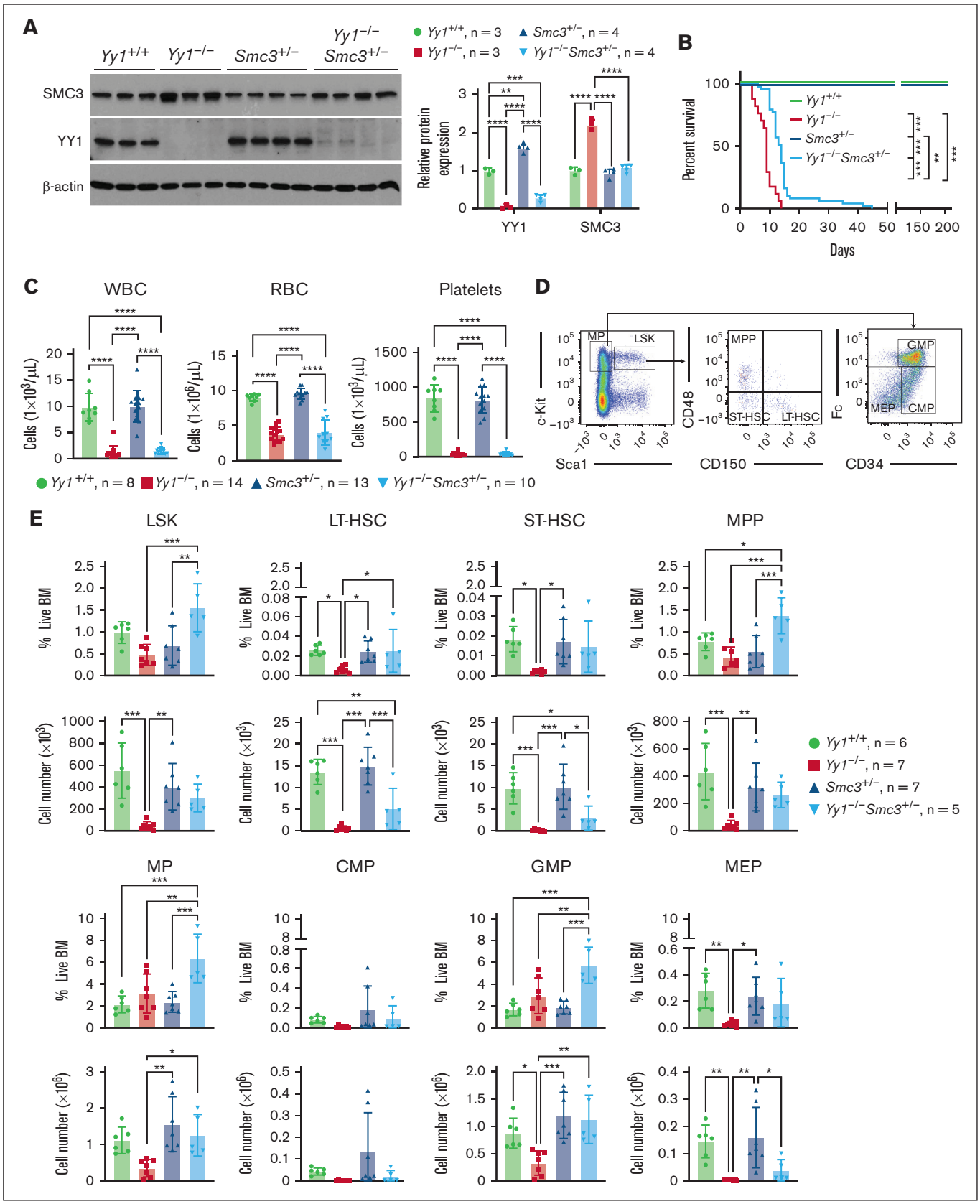

Figure 5. *Smc3* haploinsufficiency partially rescues *Yy1*$^{-/-}$ HSPC percentages and numbers. (A) SMC3 expression was normalized in *Yy1*$^{-/-}$*Smc3*$^{+/-}$ BMCs. Western blot and quantification to detect SMC3 and YY1 protein expressions in BMCs of *Yy1*$^{-/-}$, *Yy1*$^{+/+}$, *Smc3*$^{+/-}$, and *Yy1*$^{-/-}$*Smc3*$^{+/-}$ mice. (B) Survival curve

Thus, SMC3 is upregulated in YY1-deficient BMCs. Consistently, ChIP-qPCR analysis show that YY1 occupied the *Smc3* promoter area in $Yy1^{+/+}$ total BMCs but not in $Yy1^{-/-}$cells (Figure 4F). Our data support that YY1 deficiency leads to loss of YY1 binding/occupancy at the *Smc3* promoter and upregulation of SMC3.

SMC3 expression is normalized in $Yy1^{-/-}Smc3^{+/-}$ mice

Because SMC3 is upregulated in YY1-deficient HSPCs (Figure 4D-E),[17] we evaluate the functional significance of YY1 regulation of SMC3 by deleting 1 copy of *Smc3* in YY1 knockout mice. To generate $Yy1^{-/-}Smc3^{+/-}$ mice, $Yy1^{f/f}$ $Smc3^{f/f}$ mice were first generated by crossing $Yy1^{f/f}$ with $Smc3^{f/f}$ and then crossing $Yy1^{f/+}Smc3^{f/+}$ heterozygotes. $Yy1^{f/f}$ $Smc3^{f/f}$ mice were subsequently crossed with $Yy1^{f/+}$*Mx1-Cre* mice to generate $Yy1^{f/f}$ $Smc3^{f/+}$*Mx1-Cre* mice ($Yy1^{-/-}Smc3^{+/-}$; supplemental Figure 4A). After pI-pC injections, homozygous *Yy1* and heterozygous *Smc3* were selectively deleted in $Yy1^{f/f}$ $Smc3^{f/+}$ BMCs, and loxP-flanked $Yy1^{f}$ and $Smc3^{f}$ were not detected by PCR. Using DNA from tail samples as a control, we show that rearrangement/deletion events at *Yy1* and *Smc3* were specific to the hematopoietic cells (supplemental Figure 4B). *Mx1-Cre* ($Yy1^{+/+}$), $Yy1^{f/f}$ *Mx1-Cre* ($Yy1^{-/-}$), $Smc3^{f/+}$*Mx1-Cre* ($Smc3^{+/-}$), and $Yy1^{f/f}$ $Smc3^{f/+}$ *Mx1-Cre* ($Yy1^{-/-}Smc3^{+/-}$) mice were evaluated after 4 doses of pI-pC injections. Interestingly, although SMC3 was upregulated in $Yy1^{-/-}$BMCs, SMC3 protein expression was normalized to the wild-type level in $Yy1^{-/-}Smc3^{+/-}$ BMCs (Figure 5A). Thus, we concluded that SMC3 is overexpressed in YY1-deficient BMCs, and SMC3 expression level is normalized to the wild-type level in $Yy1^{-/-}Smc3^{+/-}$ mice.

Deletion of 1 *Smc3* allele partially rescues LT-HSC percentage in YY1-deficient mice

Consistent with our previously published result,[17] YY1-deficient mice died ~10 days after pI-pC injections.[17] Although $Yy1^{-/-}Smc3^{+/-}$ mice demonstrated increased survival compared with YY1-deficient mice, they still had significant survival defects compared to wild-type or $Smc3^{+/-}$ mice (Figure 5B). Similar to YY1-deficient mice, $Yy1^{-/-}Smc3^{+/-}$ mice were severely pancytopenic with reduction of red blood cells, platelets, and leukocytes (Figure 5C). Although $Yy1^{-/-}$mice had decreased numbers of LT-HSCs ($Lin^{-}Sca1^{+}c\text{-}Kit^{+}CD48^{-}CD150^{+}$), short-term HSCs (ST-HSC; $Lin^{-}Sca1^{+}c\text{-}Kit^{+}CD48^{-}CD150^{-}$), MPPs ($Lin^{-}Sca1^{+}c\text{-}Kit^{+}CD48^{+}CD150^{-}$), GMP ($Lin^{-}Sca1^{-}c\text{-}Kit^{+}CD34^{+}CD16/32^{hi}$), and MEP ($Lin^{-}Sca1^{-}c\text{-}Kit^{+}CD34^{-}CD16/32^{low}$) compared with wild-type mice, $Yy1^{-/-}Smc3^{+/-}$ mice had increased percentages of LT-HSCs, MPPs, MPs, and GMPs compared with $Yy1^{-/-}$mice. Strikingly, $Yy1^{-/-}Smc3^{+/-}$ mice had similar cell numbers of MPs and GMPs compared with wild-type mice. Thus, deletion of 1 allele of *Smc3* leads to a partial rescue of HSC and progenitor cell percentages and numbers in YY1-deficient mice (Figure 5D-E; supplemental Figure 5).

Deletion of 1 *Smc3* allele in YY1-deficient HSCs partially restores HSC quiescence

Because our previous data showed that YY1 deficiency caused decreased HSC quiescence and self-renewal,[17] we assessed the impact of deleting 1 copy of *Smc3* on HSC functions in YY1-deficient mice. In $Yy1^{-/-}Smc3^{+/-}$ mice, there was an increase in the percentage of cells in the G0 phase in LT-HSC and ST-HSC compartments when compared with $Yy1^{-/-}$HSCs (Figure 6A-C) but not in the MPP population (Figure 6D). The percentages of cells in active proliferative stages (G1 and/or S-G2-M phases) were decreased in $Yy1^{-/-}Smc3^{+/-}$ LT-HSCs and ST-HSCs compared with $Yy1^{-/-}$ HSCs. Our result showed that HSC quiescence was partially restored in $Yy1^{-/-}Smc3^{+/-}$ mice by deleting 1 copy of *Smc3* in YY1-deficient HSCs.

Next, we assessed blood chimerism in mice transplanted with *Mx1-Cre*, $Yy1^{f/f}$ *Mx1-Cre*, $Smc3^{f/+}$*Mx1-Cre*, and $Yy1^{f/f}$ $Smc3^{f/+}$*Mx1-Cre* BMCs. CD45.1 recipient mice were treated with pI-pC injections at 4 weeks after BM transplantation and donor-derived percentages (% $CD45.2^{+}$) were evaluated at 4, 8, 12, 16, and 20 weeks after BM transplant (Figure 6E). At week 4, before pI-pC injections, all 4 cohorts had similar donor-derived percentages. Beginning at week 8 (4 weeks after pI-pC injections), mice transplanted with $Yy1^{f/f}$ *Mx1-Cre* and $Yy1^{f/f}$ $Smc3^{f/+}$*Mx1-Cre* BMCs had significantly decreased donor-derived percentages in peripheral monocyte, neutrophil, and B- and T-cell compartments, compared with mice transplanted with *Mx1-Cre* or $Smc3^{f/+}$*Mx1-Cre* BMCs. Mice transplanted with $Smc3^{f/+}$*Mx1-Cre* BMCs had a higher donor-derived percentage in the myeloid compartments, as previously described[26] (Figure 6F). Our data support that both $Yy1^{-/-}$and $Yy1^{-/-}Smc3^{+/-}$ HSCs fail to reconstitute blood. Thus, restoring SMC3 expression level in YY1-deficient mice was able to partially reestablish the HSC quiescence but not the capacity to reconstitute blood.

YY1 regulates HSC metabolism via an SMC3-independent pathway

To further elucidate the underlying mechanisms of YY1 regulation of HSC functions, RNA-seq analysis was conducted in LSK cells sorted from $Yy1^{-/-}$, $Yy1^{-/-}Smc3^{+/-}$, and $Yy1^{+/+}$ mice. There were 836 upregulated and 1502 downregulated genes detected in $Yy1^{-/-}$LSK compared with $Yy1^{+/+}$ LSK cells, and there were 621 upregulated and 1370 downregulated genes detected in $Yy1^{-/-}Smc3^{+/-}$ LSK compared with $Yy1^{+/+}$ LSK cells (supplemental Figure 6). Genes involved in HSC long-term self-renewal and metabolism were enriched in pathway analysis in $Yy1^{-/-}$and $Yy1^{-/-}Smc3^{+/-}$ LSKs compared with $Yy1^{+/+}$ cells (Figure 7A). Genes involved in the immune system were enriched in pathway analysis comparing $Yy1^{-/-}Smc3^{+/-}$ with $Yy1^{-/-}$LSKs. Gene set enrichment analysis showed that pathways involved in metabolism were deregulated in both $Yy1^{-/-}$and $Yy1^{-/-}Smc3^{+/-}$ LSK cells compared with wild-type LSKs (Figure 7B). Many genes that are critical for HSC metabolism and hypoxia were dysregulated; *Hif1α,*

Figure 5 (continued) of $Yy1^{+/+}$, $Yy1^{-/-}$, $Smc3^{+/-}$, and $Yy1^{-/-}Smc3^{+/-}$ mice. (C) Complete blood count (CBC) analysis. (D) Representative flow gating strategy for LSK, LT-HSC, ST-HSC, MPP, MP, common myeloid progenitors (CMP), granulocyte monocyte progenitors (GMP), and megakaryocyte erythroid progenitors (MEP) populations. (E) Quantification of percentages and absolute numbers of LSK, LT-HSC, ST-HSC, MPP, MP, CMP, GMP and MEP populations. N represents the number of mice; data are presented as means ± SD; $^{*}P < .05$, $^{**}P < .01$, and $^{***}P < .001$.

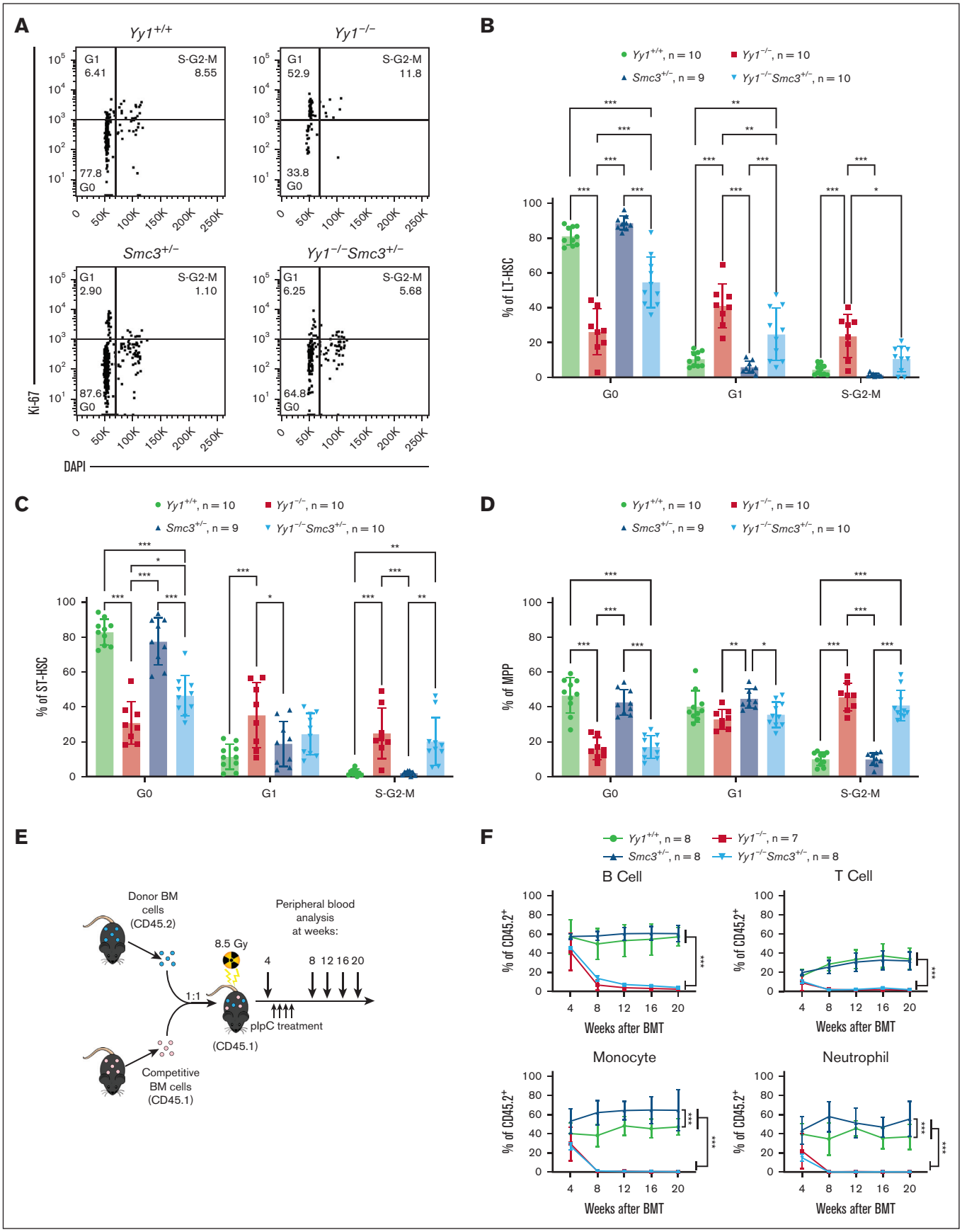
A
Yy1+/+
Yy1−/−
Smc3+/−
Yy1−/−Smc3+/−
G1
S-G2-M
G0
Ki-67
DAPI
B
Yy1+/+, n = 10
Yy1−/−, n = 10
Smc3+/−, n = 9
Yy1−/−Smc3+/−, n = 10
% of LT-HSC
G0
G1
S-G2-M
C
% of ST-HSC
D
% of MPP
E
Donor BM cells (CD45.2)
8.5 Gy
Peripheral blood analysis at weeks:
4 8 12 16 20
1:1
pIpC treatment
(CD45.1)
Competitive BM cells (CD45.1)
F
Yy1+/+, n = 8
Yy1−/−, n = 7
Smc3+/−, n = 8
Yy1−/−Smc3+/−, n = 8
B Cell
T Cell
Monocyte
Neutrophil
% of CD45.2+
Weeks after BMT

Figure 6.

Hif3α, Plekha5, Klhl3, Pfkl, Vnn1, Mdga1, Gata2, Ptgds, Sox4, and *Hoxa3* were downregulated, and *Ttll9* and *Slc4a8* were upregulated in $Yy1^{-/-}$and $Yy1^{-/-}Smc3^{+/-}$ LSK cells compared with $Yy1^{+/+}$ cells (Figure 7C-D). Based on compiled ChIP-seq analysis (Figure 1), YY1 occupied the promoter areas of *Hif1α, Hif3α, Hoxa3*, and *Pfkl* without cohesin. In contrast, YY1 colocalized with cohesin and/or CTCF at the promoters of *Sox4, Hoxa3*, and *Slc4a8* (Figure 7E). Quantitative reverse transcription PCR confirm that *Hif1α* and *Hif3α* were downregulated in $Yy1^{-/-}$LSK cells and deletion of 1 copy of *Smc3* did not restore *Hif1α* and *Hif3α* expressions in $Yy1^{-/-}Smc3^{+/-}$ LSK cells (supplemental Figure 7). Thus, YY1 controls HSC metabolic genes regardless of *Smc3* expression level. To assess gene expression changes upon acute protein deletion, we knocked down YY1 in HPC-7 cells by shRNA. Compared with sh-Luc control, *Hif3α, Plekha5*, and *Klhl3* were downregulated (supplemental Figure 8). Because *Hif1α* and *Hif3α* are critical for maintaining the proper intracellular ROS level in HSCs, we analyzed intracellular ROS levels in $Yy1^{-/-}$, $Yy1^{-/-}Smc3^{+/-}$, and $Yy1^{+/+}$ LT-HSCs ($Lin^{-}Sca1^{+}c\text{-}Kit^{+}CD48^{-}CD150^{+}$) and ST-HSCs ($Lin^{-}Sca1^{+}c\text{-}Kit^{+}CD48^{-}CD150^{-}$) by flow analysis. YY1 deficiency leads to an increase of intracellular ROS in LT-HSCs and ST-HSCs, and the increase of ROS was also detected in $Yy1^{-/-}Smc3^{+/-}$ HSCs (Figure 7F). Our results show that YY1 controls HSC metabolic genes and regulates intracellular ROS level in HSCs, and YY1 regulation of HSC ROS and metabolism is independent of the YY1–SMC3 axis.

Discussion

YY1, cohesion, and CTCF have been implicated in the formation of DNA loops needed for variable diversity joining rearrangement at the immunoglobulin locus during B-cell development.[13,45-47] Moreover, YY1 has been identified as a new critical chromatin structural factor in addition to CTCF and cohesin to mediate DNA looping and alteration of chromatin and chromosome tertiary structure.[3,48] YY1 mediates transcriptional repression through its C-terminal region that contains 4 C_2H_2-type zinc finger motifs (amino acids 298-414),[42,43] whereas the N-terminal region of YY1 (amino acids 1-200) mediates transcriptional activation.[2,42,43,49,50] YY1 recruits PcG proteins and causes consequent histone modification through a sequence motif that maps to amino acid residues 201 to 226 (the YY1REPO domain).[5] The C-terminal portion of YY1, including amino acids 201 through 414 (YY1 201-414), is critical for chromatin looping needed for immunoglobulin class switching recombination,[51] as well as for X-chromosome inactivation[52] (Figure 3F). Young et al demonstrated that YY1 binds to active enhancers and promoter-proximal elements and forms dimers that facilitate the long-distance interaction of these DNA elements.[3] Our studies here show that YY1 physically interacts with cohesin complex proteins via the C-terminal zinc finger domain (Figure 3G), and YY1 and cohesin complex proteins cooccupy a large cohort of promoters genome wide (Figures 1 and 2). Interestingly, YY1 binds at the *Smc3* promoter directly (Figure 4A,C,F; supplemental Figure 3A-B) and represses SMC3 expression (Figure 4B,D-E). Genes that were occupied by YY1 play distinct biological functions in metabolism compared with genes that were only occupied by CTCF and cohesin (Figures 1C-D and 2D). Consistent with YY1 genome-wide occupancy (Figures 1D and 2D), YY1 deficiency leads to a deregulated genetic network governing cell metabolisms (Figure 7A-D) and failure to maintain proper ROS levels in HSCs (Figure 7F). Interestingly, although SMC3 expression was normalized to the wild-type level in $Yy1^{-/-}Smc3^{+/-}$ mice, $Yy1^{-/-}Smc3^{+/-}$ HSCs fail to reconstitute blood, likely because of deregulated HSC metabolic genes and elevated ROS levels. Thus, YY1 controls HSC functions via both SMC3-dependent and -independent pathways.

One possible hypothetical model is that YY1 binds to active enhancers and promoter-proximal elements and forms heterodimers with SMC3 and/or CTCF (Figure 3),[53] or forms homodimers with itself that facilitate the formation of long-distance DNA loops.[3] Without YY1, SMC3 is upregulated (Figure 4D-E), and remains bound at most proximal promoter regions (Figure 2E). The promoter-enhancer looping is mainly maintained by cohesin interacting with other chromatin structural factors such as CTCF. Because larger chromosomal loop structures are usually made by the interaction of CTCF proteins with cohesin complex proteins,[54-57] the chromatin/DNA looping structures are altered in YY1-deficient HSCs. Because of the chromatin conformation change, genes involved in cell metabolism, which are mainly occupied by YY1 during normal conditions, remained deregulated regardless of the presence of other chromatin structural factors. Thus, YY1-deficient HSCs have decreased *Hif1α* and *Hif3α,* elevated intracellular ROS, and fail to reconstitute blood (Figure 7G). It will be interesting to further analyze high-order chromatin structures of gene loci that are critical for HSC metabolism in $Yy1^{+/+}$, $Yy1^{-/-}$, and $Yy1^{-/-}Smc3^{+/-}$ HSPCs in the future.

In adult humans, ~90% of HSCs exist in a quiescent nondividing state (G0), and up to a third of the remaining 10% of HSCs actively proliferate and are found in other stages of the cell cycle.[58-60] Quiescence is a fundamental characteristic of HSCs in adult BM, and adult HSCs can remain in a quiescent state for a prolonged time.[60] Generally, HSC cycle quiescence parallels its capacity for self-renewal and long-term repopulating activity. Thus, the cell cycle must be precisely regulated in HSCs to ensure adequate hematopoiesis without stem cell exhaustion.[61,62] Many extrinsic factors regulate and balance the processes of quiescence, self-renewal, and differentiation of HSCs[63-67]: these include proinflammatory cytokines (eg, transforming growth factor β, IFN-γ, and IFN-α)[68-70] and osteoblastic and sinusoidal vascular niches.[63-67] Moreover, the impact of extrinsic regulators is modified and modulated by intrinsic regulators of cell cycle progression in HSCs, including some transcription factors.[71-74] Our study shows that YY1 regulatory function in maintaining HSC quiescence is at least partially through its regulation of cohesin complex protein SMC3. Although YY1-deficient HSPCs are highly proliferative and have a

Figure 6. *Smc3* haploinsufficiency partially restores HSC quiescence in $Yy1^{-/-}$mice. (A) Representative gating strategy for Ki67/DAPI cell proliferation assay of LT-HSCs ($Lin^{-}Sca1^{+}c\text{-}Kit^{+}CD48^{-}CD150^{+}$). Cells in the G0 phase were defined as $Ki67^{-}DAPI^{-}$. Cells in the G1 phase were defined as $Ki67^{+}DAPI^{-}$. Cells in S/G2/M phase were defined as $Ki67^{+}DAPI^{+}$. (B-D) Quantification of percentages of LT-HSC, ST-HSC, and MPP cells in G0, G1, and S/G2/M phase. (E) Experimental strategy of BM transplantation (BMT). (F) Quantification of donor-derived contribution in B-cell ($Thy1.2^{-}CD19^{+}$), T-cell ($Thy1.2^{+}CD19^{-}$), monocyte ($Mac1^{+}Gr1^{-}$), and neutrophil ($Mac1^{+}Gr1^{+}$) populations at 4, 8, 12, 16, and 20 weeks after BMT. N represents the number of mice; data are presented as means ± SD; $^{*}P < .05$, $^{**}P < .01$, and $^{***}P < .001$.

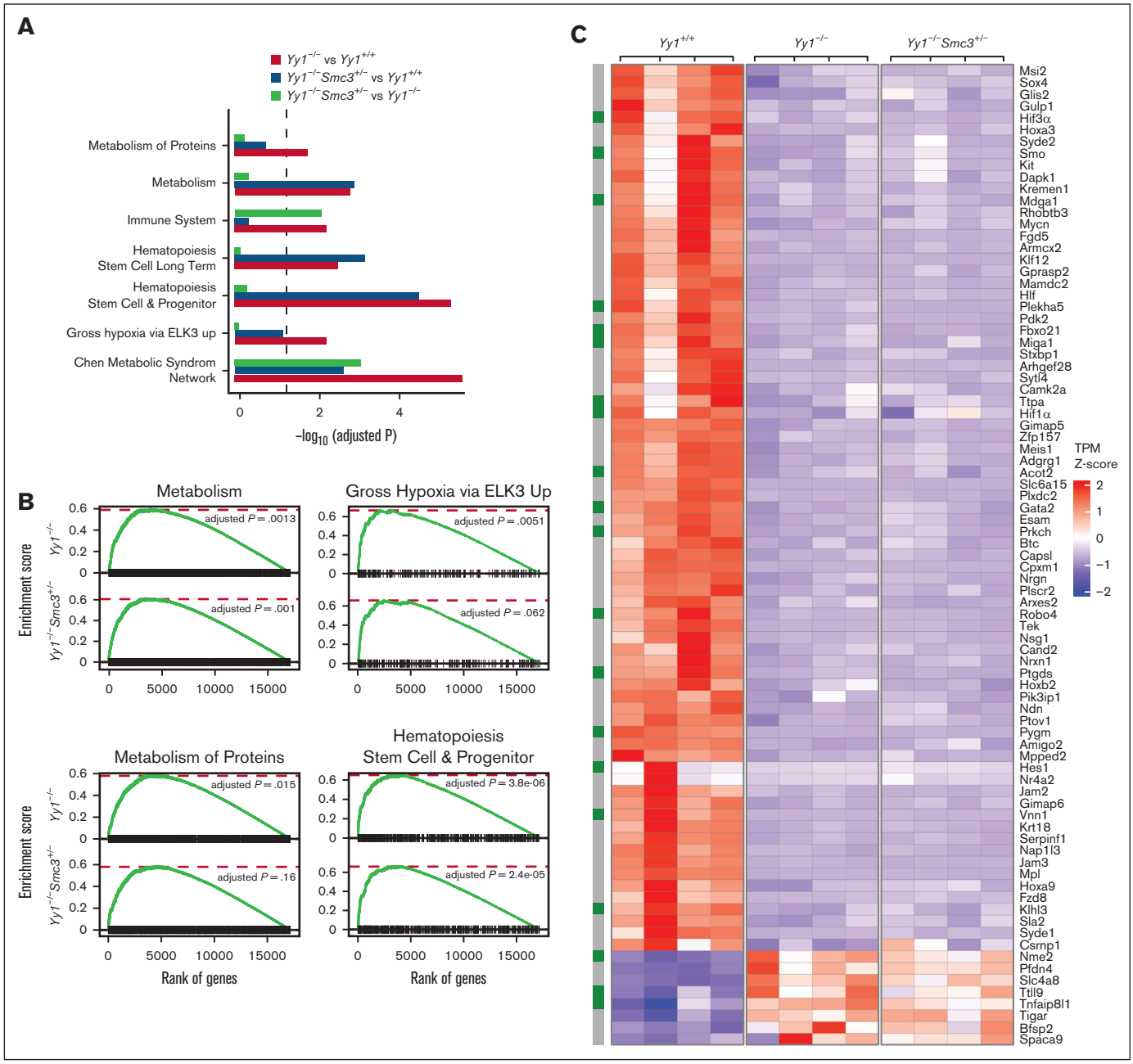

Figure 7. *Yy1*$^{-/-}$LSKs exhibit an aberrant genetic network with corruption of genes involved in HSC metabolism. RNA-seq–based comparison of gene expression in sorted *Yy1*$^{+/+}$, *Yy1*$^{-/-}$, and *Yy1*$^{-/-}$*Smc3*$^{+/-}$ LSK cells. (A-B) Gene set enrichment analysis of genes deregulated in *Yy1*$^{-/-}$vs *Yy1*$^{+/+}$, *Yy1*$^{-/-}$*Smc3*$^{+/-}$ vs *Yy1*$^{+/+}$, and *Yy1*$^{-/-}$*Smc3*$^{+/-}$ vs *Yy1*$^{-/-}$. Enriched biological processes are shown with corresponding adjusted *P* values (A). Genes involved in metabolism and HSPCs are enriched in *Yy1*$^{-/-}$and *Yy1*$^{-/-}$*Smc3*$^{+/-}$ LSK cells compared with *Yy1*$^{+/+}$ (B). (C) Heat map depicting selected upregulated and downregulated genes involved in regulation of HSPC function based on transcript per million. The green boxes label the genes involved in metabolism pathway. (D) mRNA expression levels of genes that are critical for metabolism and HSC functions based on the transcript per million of RNA-seq. (E) YY1, cohesion, and CTCF occupancy at the promoters of genes that are critical for HSC function and metabolism. (F) Increased intracellular ROS levels in *Yy1*$^{-/-}$and *Yy1*$^{-/-}$*Smc3*$^{+/-}$ HSCs. (G) Schematic diagram shows that YY1 represses SMC3 expression and interacts with SMC3 to facilitate chromatin structures of genes that are critical for HSC metabolism. In YY1-deficient HSCs, SMC3 is upregulated and interacts with CTCF, which leads to changes of chromatin conformation and altered metabolic gene expression. N represents the number of mice; data are presented as means ± SD; **P* < .05 ***P* < .01, and ****P* < .001.

high SMC3 expression level, normalizing SMC3 expression level in YY1-deficient mice is able to partially restore HSC quiescence (Figure 6A-D). Although HSC quiescence was partially restored in *Yy1*$^{-/-}$*Smc3*$^{+/-}$ mice, *Yy1*$^{-/-}$*Smc3*$^{+/-}$ HSCs fail to reconstitute blood upon BM transplant (Figure 6E-F). Therefore, YY1 regulation of cohesin is a critical driver for HSC quiescence but not for all HSC functions. Although genes/pathways that are critical for cell metabolism are deregulated in both *Yy1*$^{-/-}$and *Yy1*$^{-/-}$*Smc3*$^{+/-}$

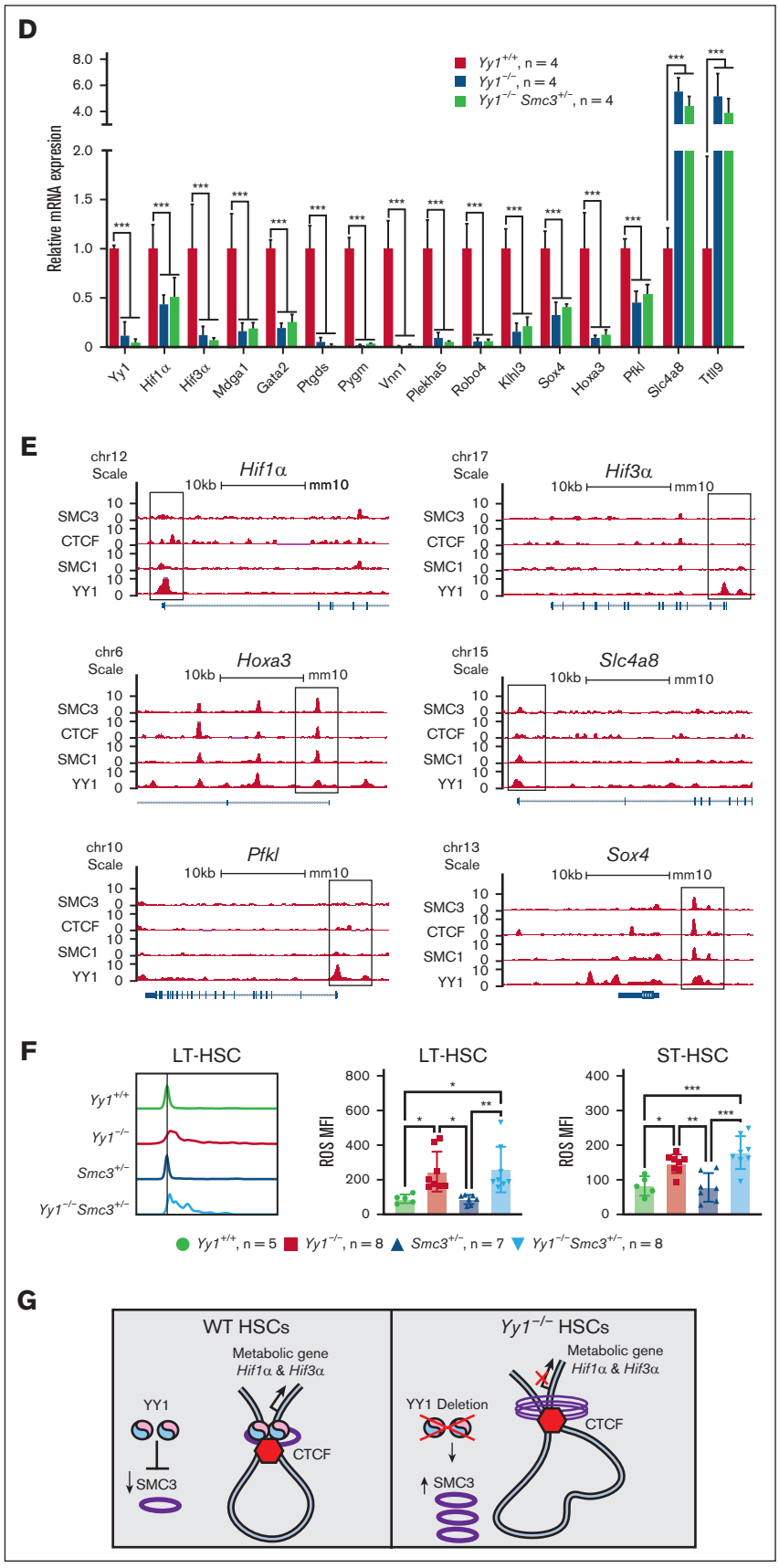

Figure 7 (continued)

samples, pathway analysis show that genes involved in immune system are differently regulated in $Yy1^{-/-}$and $Yy1^{-/-}Smc3^{+/-}$ cells (Figure 7A). SMC3 occupancy at the promoter regions, which are critical for cell metabolism, heavily rely on presence of YY1 (Figure 2F), and this may explain why normalization of SMC3 expression is not sufficient to rescue HSC metabolic defects. It will be interesting to further dissect how the YY1–SMC3 axis controls the cross talk between HSCs and the immune system, such as immune cells in the BM microenvironment, in the future.

Acknowledgments

The authors thank the University of Wisconsin Carbone Comprehensive Cancer Center for use of its Shared Services (Flow Cytometry Core and Cancer Informatics Shared Resources), which are supported by University of Wisconsin Carbone Comprehensive Cancer Center grant P30 CA014520, to complete this research. The authors thank Ross Levine for providing $Smc3^{f/f}$ mice.

This work was supported by National Institutes of Health Office of Infrasture grant R03OD026603 and National Heart, Lung, and Blood Institute grant R01HL146540 (X.P.), and the Coordination for the Improvement of High Education Personnel, Brazil (A.L.F.V.A.). A.D.V. is supported by a National Cancer Institute career development grant K08 CA215317 and a grant from the Edward P. Evans Foundation.

Authorship

Contribution: X.P. designed experiments; Z.L., A.L.F.V.A., Y.W., S.S., A.K., and X.P. performed experiments; Z.L., A.L.F.V.A., Y.W., P.L., S.J.M., A.D.V., M.B., and X.P. analyzed and interpreted the data; and Z.L., Y.W., A.L.F.V.A., P.L., and X.P. wrote the manuscript.

Conflict-of-interest disclosure: The authors declare no competing financial interests.

ORCID profiles: P.L., 0000-0001-5655-2259; A.K., 0009-0005-5557-2473; S.J.M., 0000-0002-3820-8400; A.D.V., 0000-0001-7039-0110; M.B., 0000-0001-8915-8012; X.P., 0000-0002-8308-8495.

Correspondence: Xuan Pan, Department of Medical Sciences, University of Wisconsin-Madison Medical Sciences, 2015 Linden Dr, 4470 SVM, Madison, WI 53706; email: xpan24@wisc.edu.

References

1. Park K, Atchison ML. Isolation of a candidate repressor/activator, NF-E1 (YY-1, d), that binds to the immunoglobulin k 3' enhancer and the immunoglobulin heavy-chain mE1 site. *Proc Natl Acad Sci U S A*. 1991;88(21):9804-9808.
2. Shi Y, Seto E, Chang L-S, Shenk T. Transcriptional repression by YY1, a human GLI-Kruppel-related protein, and relief of repression by adenovirus E1A protein. *Cell*. 1991;67(2):377-388.
3. Weintraub AS, Li CH, Zamudio AV, et al. YY1 is a structural regulator of enhancer-promoter loops. *Cell*. 2017;171(7):1573-1588.
4. Beagan JA, Duong MT, Titus KR, et al. YY1 and CTCF orchestrate a 3D chromatin looping switch during early neural lineage commitment. *Genome Res*. 2017;27(7):1139-1152.
5. Wilkinson FH, Park K, Atchison ML. Polycomb recruitment to DNA in vivo by the YY1 REPO domain. *Proc Natl Acad Sci U S A*. 2006;103(51):19296-19301.
6. Srinivasan L, Atchison ML. YY1 DNA binding and PcG recruitment requires CtBP. *Genes Dev*. 2004;18(21):2596-2601.
7. Atchison L, Ghias A, Wilkinson F, Bonini N, Atchison ML. The YY1 transcription factor functions as a PcG protein in vivo. *EMBO J*. 2003;22(6):1347-1358.
8. Liu H, Schmidt-Supprian M, Shi Y, et al. Yin Yang 1 is a critical regulator of B-cell development. *Genes Dev*. 2007;21(10):1179-1189.
9. Majewski IJ, Ritchie ME, Phipson B, et al. Opposing roles of polycomb repressive complexes in hematopoietic stem and progenitor cells. *Blood*. 2010;116(5):731-739.
10. Castellano G, Torrisi E, Ligresti G, et al. Yin Yang 1 overexpression in diffuse large B-cell lymphoma is associated with B-cell transformation and tumor progression. *Cell Cycle*. 2010;9(3):557-563.
11. Wang W, Qiao S, Li G, et al. A histidine cluster determines YY1-compartmentalized coactivators and chromatin elements in phase-separated enhancer clusters. *Nucleic Acids Res*. 2022;50(9):4917-4937.
12. Kleiman E, Jia H, Loguercio S, Su AI, Feeney AJ. YY1 plays an essential role at all stages of B-cell differentiation. *Proc Natl Acad Sci U S A*. 2016;113(27):E3911-3920.
13. Pan X, Papasani M, Hao Y, et al. YY1 controls Igkappa repertoire and B-cell development, and localizes with condensin on the Igkappa locus. *EMBO J*. 2013;32(8):1168-1182.
14. Zaprazna K, Atchison ML. YY1 controls immunoglobulin class switch recombination and nuclear activation-induced deaminase levels. *Mol Cell Biol*. 2012;32(8):1542-1554.
15. Chen L, Foreman DP, Sant'Angelo DB, Krangel MS. Yin Yang 1 promotes thymocyte survival by downregulating p53. *J Immunol*. 2016;196(6):2572-2582.
16. Assumpcao A, Fu G, Singh DK, et al. A lineage-specific requirement for YY1 polycomb group protein function in early T cell development. *Development*. 2021;148(7):dev197319.
17. Lu Z, Hong CC, Kong G, et al. Polycomb group protein YY1 is an essential regulator of hematopoietic stem cell quiescence. *Cell Rep*. 2018;22(6):1545-1559.

18. Losada A. Cohesin in cancer: chromosome segregation and beyond. *Nat Rev Cancer*. 2014;14(6):389-393.
19. Haering CH, Lowe J, Hochwagen A, Nasmyth K. Molecular architecture of SMC proteins and the yeast cohesin complex. *Mol Cell*. 2002;9(4):773-788.
20. Schockel L, Mockel M, Mayer B, Boos D, Stemmann O. Cleavage of cohesin rings coordinates the separation of centrioles and chromatids. *Nat Cell Biol*. 2011;13(8):966-972.
21. Heidinger-Pauli JM, Mert O, Davenport C, Guacci V, Koshland D. Systematic reduction of cohesin differentially affects chromosome segregation, condensation, and DNA repair. *Curr Biol*. 2010;20(10):957-963.
22. Wutz G, Várnai C, Nagasaka K, et al. Topologically associating domains and chromatin loops depend on cohesin and are regulated by CTCF, WAPL, and PDS5 proteins. *EMBO J*. 2017;36(24):3573-3599.
23. Mullenders J, Aranda-Orgilles B, Lhoumaud P, et al. Cohesin loss alters adult hematopoietic stem cell homeostasis, leading to myeloproliferative neoplasms. *J Exp Med*. 2015;212(11):1833-1850.
24. Galeev R, Baudet A, Kumar P, et al. Genome-wide RNAi screen identifies cohesin genes as modifiers of renewal and differentiation in human HSCs. *Cell Rep*. 2016;14(12):2988-3000.
25. Mazumdar C, Shen Y, Xavy S, et al. Leukemia-associated cohesin mutants dominantly enforce stem cell programs and impair human hematopoietic progenitor differentiation. *Cell Stem Cell*. 2015;17(6):675-688.
26. Viny AD, Ott CJ, Spitzer B, et al. Dose-dependent role of the cohesin complex in normal and malignant hematopoiesis. *J Exp Med*. 2015;212(11):1819-1832.
27. Bonev B, Cavalli G. Organization and function of the 3D genome. *Nat Rev Genet*. 2016;17(12):772.
28. de Laat W, Duboule D. Topology of mammalian developmental enhancers and their regulatory landscapes. *Nature*. 2013;502(7472):499-506.
29. Spitz F. Gene regulation at a distance: from remote enhancers to 3D regulatory ensembles. *Semin Cell Dev Biol*. 2016;57(4):57-67.
30. Levine M, Cattoglio C, Tjian R. Looping back to leap forward: transcription enters a new era. *Cell*. 2014;157(1):13-25.
31. Handoko L, Xu H, Li G, et al. CTCF-mediated functional chromatin interactome in pluripotent cells. *Nat Genet*. 2011;43(7):630-638.
32. Phillips JE, Corces VG. CTCF: master weaver of the genome. *Cell*. 2009;137(7):1194-1211.
33. Sofueva S, Yaffe E, Chan WC, et al. Cohesin-mediated interactions organize chromosomal domain architecture. *EMBO J*. 2013;32(24):3119-3129.
34. Hadjur S, Williams LM, Ryan NK, et al. Cohesins form chromosomal cis-interactions at the developmentally regulated IFNG locus. *Nature*. 2009;460(7253):410-413.
35. Viny AD, Bowman RL, Liu Y, et al. Cohesin members Stag1 and Stag2 display distinct roles in chromatin accessibility and topological control of HSC self-renewal and differentiation. *Cell Stem Cell*. 2019;25(5):682-696.e8.
36. Kagey MH, Newman JJ, Bilodeau S, et al. Mediator and cohesin connect gene expression and chromatin architecture. *Nature*. 2010;467(7314):430-435.
37. Ji X, Dadon DB, Abraham BJ, et al. Chromatin proteomic profiling reveals novel proteins associated with histone-marked genomic regions. *Proc Natl Acad Sci U S A*. 2015;112(12):3841-3846.
38. Sigova AA, Abraham BJ, Ji X, et al. Transcription factor trapping by RNA in gene regulatory elements. *Science*. 2015;350(6263):978-981.
39. Li Y, Nakka K, Olender T, et al. Chromatin and transcription factor profiling in rare stem cell populations using CUT&Tag. *STAR Protoc*. 2021;2(3):100751.
40. Pinto do O P, Kolterud A, Carlsson L. Expression of the LIM-homeobox gene LH2 generates immortalized steel factor-dependent multipotent hematopoietic precursors. *EMBO J*. 1998;17(19):5744-5756.
41. Wilson NK, Schoenfelder S, Hannah R, et al. Integrated genome-scale analysis of the transcriptional regulatory landscape in a blood stem/progenitor cell model. *Blood*. 2016;127(13):e12-23.
42. Bushmeyer S, Park K, Atchison ML. Characterization of functional domains within the multifunctional transcription factor, YY1. *J Biol Chem*. 1995;270(50):30213-30220.
43. Bushmeyer SM, Atchison ML. Identification of YY1 sequences necessary for association with the nuclear matrix and for transcriptional repression functions. *J Cell Biochem*. 1998;68(4):484-499.
44. Gordon S, Akopyan G, Garban H, Bonavida B. Transcription factor YY1: structure, function, and therapeutic implications in cancer biology. *Oncogene*. 2006;25(8):1125-1142.
45. Degner SC, Verma-Gaur J, Wong TP, et al. CCCTC-binding factor (CTCF) and cohesin influence the genomic architecture of the Igh locus and antisense transcription in pro-B cells. *Proc Natl Acad Sci U S A*. 2011;108(23):9566-9571.
46. Degner SC, Wong TP, Jankevicius G, Feeney AJ. Cutting edge: developmental stage-specific recruitment of cohesin to CTCF sites throughout immunoglobulin loci during B lymphocyte development. *J Immunol*. 2009;182(1):44-48.
47. Ribeiro de Almeida C, Stadhouders R, de Bruijn MJW, et al. The DNA-binding protein CTCF limits proximal Vkappa recombination and restricts kappa enhancer interactions to the immunoglobulin kappa light chain locus. *Immunity*. 2011;35(4):501-513.
48. Li L, Williams P, Ren W, et al. YY1 interacts with guanine quadruplexes to regulate DNA looping and gene expression. *Nat Chem Biol*. 2021;17(2):161-168.

49. Flanagan JR, Becker KG, Ennist DL, et al. Cloning of a negative transcription factor that binds to the upstream conserved region of Moloney murine leukemia virus. *Mol Cell Biol*. 1992;12(1):38-44.
50. Hariharan N, Kelley DE, Perry RPd. Delta a transcription factor that binds to downstream elements in several polymerase II promoters, is a functionally diverse zinc finger protein. *Proc Natl Acad Sci U S A*. 1991;88(21):9799-9803.
51. Mehra P, Gerasimova T, Basu A, et al. YY1 controls Emu-3'RR DNA loop formation and immunoglobulin heavy chain class switch recombination. *Blood Adv*. 2016;1(1):15-20.
52. Syrett CM, Sindhava V, Hodawadekar S, et al. Loss of Xist RNA from the inactive X during B cell development is restored in a dynamic YY1-dependent two-step process in activated B cells. *PLoS Genet*. 2017;13(10):e1007050.
53. Donohoe ME, Zhang L-F, Xu N, Shi Y, Lee JT. Identification of a Ctcf cofactor, YY1, for the X chromosome binary switch. *Mol Cell*. 2007;25(1):43-56.
54. Gibcus JH, Dekker J. The hierarchy of the 3D genome. *Mol Cell*. 2013;49(5):773-782.
55. Gorkin DU, Leung D, Ren B. The 3D genome in transcriptional regulation and pluripotency. *Cell Stem Cell*. 2014;14(6):762-775.
56. Merkenschlager M, Nora EP. CTCF and cohesin in genome folding and transcriptional gene regulation. *Annu Rev Genomics Hum Genet*. 2016;17(1):17-43.
57. Gabriele M, Brandão HB, Grosse-Holz S, et al. Dynamics of CTCF- and cohesin-mediated chromatin looping revealed by live-cell imaging. *Science*. 2022;376(6592):496-501.
58. Goodell MA, Brose K, Paradis G, Conner AS, Mulligan RC. Isolation and functional properties of murine hematopoietic stem cells that are replicating in vivo. *J Exp Med*. 1996;183(4):1797-1806.
59. Cheshier SH, Morrison SJ, Liao X, Weissman IL. In vivo proliferation and cell cycle kinetics of long-term self-renewing hematopoietic stem cells. *Proc Natl Acad Sci U S A*. 1999;96(6):3120-3125.
60. Pietras EM, Warr MR, Passegue E. Cell cycle regulation in hematopoietic stem cells. *J Cell Biol*. 2011;195(5):709-720.
61. Orford KW, Scadden DT. Deconstructing stem cell self-renewal: genetic insights into cell-cycle regulation. *Nat Rev Genet*. 2008;9(2):115-128.
62. Yang Y, Kueh AJ, Grant ZL, et al. The histone lysine acetyltransferase HBO1 (KAT7) regulates hematopoietic stem cell quiescence and self-renewal. *Blood*. 2022;139(6):845-858.
63. Kiel MJ, Morrison SJ. Maintaining hematopoietic stem cells in the vascular niche. *Immunity*. 2006;25(6):862-864.
64. Yin T, Li L. The stem cell niches in bone. *J Clin Invest*. 2006;116(5):1195-1201.
65. Zhang J, Niu C, Ye L, et al. Identification of the hematopoietic stem cell niche and control of the niche size. *Nature*. 2003;425(6960):836-841.
66. Ding L, Saunders TL, Enikolopov G, Morrison SJ. Endothelial and perivascular cells maintain hematopoietic stem cells. *Nature*. 2012;481(7382):457-462.
67. Calvi LM, Adams GB, Weibrecht KW, et al. Osteoblastic cells regulate the hematopoietic stem cell niche. *Nature*. 2003;425(6960):841-846.
68. Baldridge MT, King KY, Boles NC, Weksberg DC, Goodell MA. Quiescent hematopoietic stem cells are activated by IFN-gamma in response to chronic infection. *Nature*. 2010;465(7299):793-797.
69. Essers MA, Offner S, Blanco-Bose WE, et al. IFN alpha activates dormant hematopoietic stem cells in vivo. *Nature*. 2009;458(7240):904-908.
70. Brenet F, Kermani P, Spektor R, Rafii S, Scandura JM. TGFbeta restores hematopoietic homeostasis after myelosuppressive chemotherapy. *J Exp Med*. 2013;210(3):623-639.
71. Matsumoto A, Takeishi S, Kanie T, et al. p57 is required for quiescence and maintenance of adult hematopoietic stem cells. *Cell Stem Cell*. 2011;9(3):262-271.
72. Zou P, Yoshihara H, Hosokawa K, et al. p57(Kip2) and p27(Kip1) cooperate to maintain hematopoietic stem cell quiescence through interactions with Hsc70. *Cell Stem Cell*. 2011;9(3):247-261.
73. Lacombe J, Herblot S, Rojas-Sutterlin S, et al. Scl regulates the quiescence and the long-term competence of hematopoietic stem cells. *Blood*. 2010;115(4):792-803.
74. Wilson NK, Foster SD, Wang X, et al. Combinatorial transcriptional control in blood stem/progenitor cells: genome-wide analysis of ten major transcriptional regulators. *Cell Stem Cell*. 2010;7(4):532-544.